Pergamon

Int. J. Heat Mass Transfer. Vol. 37, No. 17, pp. 2615–2626, 1994

0017-9310/94 $7.00+0.00

0017-9310(94)E0102-Z

Green's function solution for thermal wave equation in finite bodies

A. HAJI-SHEIKH

Department of Mechanical and Aerospace Engineering, The University of Texas at Arlington, Arlington, TX 76019-0023, U.S.A.

and

J. V. BECK

Department of Mechanical Engineering, Michigan State University, East Lansing, MI 48824-1226, U.S.A.

(*Received* 1 *July* 1993 *and in final form* 24 *March* 1994)

Abstract—The classical diffusion theory is based on the assumption of local thermal equilibrium. For conduction in thin films or at low temperature, the classical theory of heat conduction breaks down. Various investigations have shown that a wave-type conduction equation adequately describes the thermal energy transport. This paper describes a general solution technique when the wave nature of thermal energy transport is dominant. The solution for temperature distribution is derived for finite bodies. The definition of Green's functions for a wave-type conduction equation is presented and a general form of the Green's function solution method for finite bodies is introduced.

INTRODUCTION

THE EXISTENCE of a thermal wave in super fluids near absolute zero has been known for decades [1]. Baumeister and Hamill [2, 3] studied thermal wave propagation in a semi-infinite solid subject to step change in the surface temperature. Ozisik and Vick [4] studied the reflection of a thermal wave in a one-dimensional slab. This subject has been intensely studied by numerous investigators and results of various investigations are available in the literature. An extensive survey of published work is beyond the scope of this paper; however, an excellent up-to-date survey of published work is reported by Ozisik and Tzou [5].

The solutions for wave-type conduction equations are generally reported for infinite bodies. Ozisik and Vick [4] presented a solution for wave propagation in a slab bounded by two insulated surfaces. This paper describes a method of solution of the thermal wave equation in many finite bodies that accept solutions for the classical diffusion equation. Solutions can be derived from the classical Green's functions. Because the classical Green's function is predictable, the solution of the wave-type conduction equation is readily available using the tabulated values [6] of the classical Green's functions [7]. The solution presented in this paper leads to a short-cut procedure that would preempt the need for lengthy mathematical derivations.

It is shown that a solution of the Fourier-type diffusion equation serves as the building block to construct a solution for the thermal wave equation. Following mathematical formulations, examples demonstrate the procedure. The numerical study shows that the convergence of the series solutions is relatively slow. A procedure to accelerate the convergence of the Green's function is presented.

MATHEMATICAL STEPS

This presentation describes a generalized solution of the heat conduction equation in the wave form [5]

$$\nabla \cdot [\mathrm{k}\nabla T(\mathbf{r}, t)] + \bar{g}(\mathbf{r}, t) = \rho c_\mathrm{p} \frac{\partial T(\mathbf{r}, t)}{\partial t} + \frac{k}{\sigma^2} \frac{\partial^2 T(\mathbf{r}, t)}{\partial t^2} \quad (1)$$

where

$$\bar{g}(\mathbf{r}, t) = g(\mathbf{r}, t) + \frac{\alpha}{\sigma^2} \frac{\partial g(\mathbf{r}, t)}{\partial t}. \quad (2)$$

The function $g(\mathbf{r}, t)$ represents an internal heat source. The heat source can be a distributed or a discrete function of position and time. The solution for equation (1) is derived from the classical Fourier-type conduction equation. The fundamental solution of the Fourier heat equation

$$\nabla \cdot [k\nabla \bar{T}(\mathbf{r}, t)] = \rho c_\mathrm{p} \frac{\partial \bar{T}(\mathbf{r}, t)}{\partial t} \quad (3)$$

in a finite body subject to homogeneous boundary conditions is

NOMENCLATURE

- b radius, m
- B_1, B_2 constants of integration
- C_{1n}, C_{2n} constants of integration
- c_p specific heat [J kg^{-1} K^{-1}]
- F_n eigenfunction
- $g(\mathbf{r}, t)$ volumetric heat source [W m^{-3}]
- $\bar{g}$ see equation (2)
- $g_n^*(t)$ function of time, see equation (11)
- $\bar{g}_n^*(t)$ Laplace transform of $g_n^*(t)$
- $G(\cdot)$ Green's function for diffusion equation
- $G_w(\cdot)$ Green's function for thermal wave equation
- $G_{wa}(\cdot)$ a-conjugate component of G_w
- $G_{wb}(\cdot)$ b-conjugate component of G_w
- k thermal conductivity [W m^{-1} K^{-1}]
- L thickness of slab [m]
- l, m, n, p indices
- N_n norm, defined by equation (8)
- q heat flux [W m^{-2}]
- r, r' radial coordinates [m]
- $\mathbf{r}$ position vector [m]
- $\mathbf{r}'$ position vector for source in Green's function [m]
- $\mathbf{r}^*$ dummy variable [m]
- s Laplace transform variable
- T temperature in thermal wave equation [K]
- $\bar{T}$ temperature in Fourier diffusion equation [K]
- T^* auxiliary temperature function [K]
- T_0 effect of initial conditions on T [K]
- T_G effect of source on T [K]
- T_B effect of boundary condition on T [K]
- T_{ii} $\partial T/\partial t$ at $t = 0$
- T_i T at $t = 0$
- t time [s]
- V volume [m^3]
- x, y, z coordinate [m]
- x', y', z' coordinates of the source in Green's function [m].

Greek symbols

- α thermal diffusivity [m^2 s^{-1}]
- β_n defined by equation (10)
- γ eigenvalue [s^{-1}]
- δ delta function
- $\mu_{m\nu}$ eigenvalues, roots of $J_\nu(\mu_{m\nu}) = 0$
- ν eigenvalue
- ξ coordinate of thermal pulse [m]
- ρ density [kg m^{-3}]
- σ speed of wave [m s^{-1}]
- τ time of the source in Green's function
- ϕ angular coordinate
- ϕ' angular coordinate of source
- $\psi_n(t)$ time function in the solution
- $\omega_n(s)$ Laplace transform of $\psi_n(t)$
- ω_n $\sqrt{\beta_n^2-\gamma_n^2}$.

$$\bar{T}(\mathbf{r}, t) = \sum_{n=1}^{\infty} F_n(\mathbf{r})e^{-\gamma_n t}. \tag{4}$$

The eigenfunction $F_n(\mathbf{r})$ satisfies the relation

$$\nabla\cdot[k\nabla F_n(\mathbf{r})] = -\gamma_n \rho c_p F_n(\mathbf{r}). \tag{5}$$

The following derivations show that the solution of equation (1) is a modified form of equation (4):

Solution of the wave equation. A solution for equation (1) is considered by modifying equation (4):

$$T = T^* + \sum_{n=1}^{\infty} \psi_n(t)F_n(\mathbf{r})e^{-\gamma_n t}. \tag{6}$$

This solution includes an unknown function of time, $\psi(t)$. The parameter $\gamma_n t$ is the apparent damping factor while the actual damping factor includes the contribution of $\psi(t)$. The computation of function $\psi(t)$ is the subject of this mathematical formulation. The function $T^* = T^*(\mathbf{r}, t)$ is any known differentiable function that satisfies the non-homogeneous boundary conditions. Further discussions on the nature of the function T^* appear later. Substitution of T from equation (6) in equation (1) yields

$$\nabla\cdot(k\nabla T^*) + \sum_{n=1}^{\infty} \nabla\cdot[k\nabla F_n(\mathbf{r})]\psi_n e^{-\gamma_n t}$$

$$+\bar{g} = \rho c_p \frac{\partial T^*}{\partial t} + \frac{k}{\sigma^2}\frac{\partial^2 T^*}{\partial t^2} + \rho c_p \sum_{n=1}^{\infty} F_n(\mathbf{r})$$

$$\times\left[-\gamma_n\psi_n e^{-\gamma_n t} + \frac{d\psi_n}{dt}e^{-\gamma_n t}\right] + \frac{k}{\sigma^2}\sum_{n=1}^{\infty} F_n(\mathbf{r})$$

$$\times\left[\gamma_n^2\psi_n e^{-\gamma_n t} - 2\gamma_n\frac{d\psi_n}{dt}e^{-\gamma_n t} + \frac{d^2\psi_n}{dt^2}e^{-\gamma_n t}\right]. \tag{7}$$

Now, one can use equation (5) to eliminate $\nabla\cdot[k\nabla F_n(\mathbf{r})]\psi_n e^{-\gamma_n t}$ on the left-hand side and $\rho c_p F_n(\mathbf{r})\gamma_n\psi_n e^{-\gamma_n t}$ on the right-hand side of equation (7). Next, multiply both sides of equation (7) by $F_m(\mathbf{r})$ and integrate over the domain. The orthogonality condition requires that

$$\int_V F_n(\mathbf{r})F_m(\mathbf{r})\,dV = \begin{cases} 0 \text{ when } n \neq m \\ N_n \text{ when } n = m \end{cases}. \tag{8}$$

The result is

$$e^{\gamma_n t}\int_V \left[\bar{g}(\mathbf{r},t)+\nabla\cdot(k\nabla T^*(\mathbf{r},t)) - \rho c_p \frac{\partial T^*(\mathbf{r},t)}{\partial t} - \frac{k}{\sigma^2}\frac{\partial^2 T^*(\mathbf{r},t)}{\partial t^2}\right]F_n(\mathbf{r})\,dV = \rho c_p N_n \dot{\psi}_n + \frac{kN_n}{\sigma^2}\left[\ddot{\psi}_n - 2\gamma_n\dot{\psi}_n + \gamma_n^2\psi_n\right] \quad (9)$$

where $\dot{\psi}_n$ and $\ddot{\psi}_n$ stand for $d\psi_n/dt$ and $d^2\psi_n/dt^2$, respectively. Equation (9) is a second-order ordinary differential equation,

$$\ddot{\psi}_n - 2\beta_n\dot{\psi}_n + \gamma_n^2\psi_n = g_n^*(t); \quad \beta_n = \gamma_n - \frac{\sigma^2}{2\alpha} \quad (10)$$

where $g_n^*(t)$ is a function of time that incorporates the effect of the internal heat source in the solution, which is σ^2/kN_n multiplied by the left side of equation (9),

$$g_n^*(t) = \frac{\sigma^2 e^{\gamma_n t}}{kN_n}\int_V \left[\bar{g}+\nabla\cdot(k\nabla T^*) - \rho c_p\frac{\partial T^*}{\partial t} - \frac{k}{\sigma^2}\frac{\partial^2 T^*}{\partial t^2}\right]F_n(\mathbf{r})\,dV \quad (11)$$

where $\bar{g} = \bar{g}(\mathbf{r},t)$ and $T^* = T^*(\mathbf{r},t)$.

Integration of ordinary differential equation

The differential equation given by equation (10) has an exact integration. The solution using the Laplace transform method is presented here to facilitate the subsequent mathematical derivations. Defining the function $\tilde{\psi}_n(s)$ as the Laplace transform $\psi_n(t)$ and $\tilde{g}_n^*(s)$ as the Laplace transform of $g_n^*(t)$, equation (10) gives the function $\tilde{\psi}_n(s)$ as

$$\tilde{\psi}_n(s) = \frac{\tilde{g}_n^*(s)}{s^2-2\beta_n s+\gamma_n^2} + \frac{s\psi_n(0)+\dot{\psi}_n(0)-2\beta_n\psi_n(0)}{s^2-2\beta_n s+\gamma_n^2}. \quad (12)$$

The denominators are the same and have two distinct roots

$$s_1 = \beta_n + \sqrt{\beta_n^2-\gamma_n^2} \quad \text{and} \quad s_2 = \beta_n - \sqrt{\beta_n^2-\gamma_n^2}. \quad (13)$$

The function $\tilde{\psi}_n(s)$, equation (12), can be written as

$$\tilde{\psi}_n(s) = \frac{\tilde{g}_n^*(s)}{2\sqrt{\beta_n^2-\gamma_n^2}}\left(\frac{1}{s-s_1}-\frac{1}{s-s_2}\right) + \frac{B_1}{s-s_1} + \frac{B_2}{s-s_2} \quad (14)$$

where B_1 and B_2 are constants. The inverse transform using the convolution theorem is

$$\psi_n(t) = \int_0^t \frac{e^{s_1(t-\tau)}-e^{s_2(t-\tau)}}{2\sqrt{\beta_n^2-\gamma_n^2}}g^*(\tau)\,d\tau + B_1 e^{s_1 t} + B_2 e^{s_2 t}. \quad (15)$$

When $\beta_n^2-\gamma_n^2 \geqslant 0$, the values of s_1 and s_2 are real; otherwise, these roots are complex. The real roots correspond to the case when $\gamma_n\alpha/\sigma^2 < 1/4$ and the complex roots are for $\gamma_n\alpha/\sigma^2 > 1/4$. The parameter α/σ^2 is the relaxation time [8] and $\gamma_n(\alpha/\sigma^2) = 1/4$ is a condition that governs the transition of a thermal wave from over- to under-damped wave modes. Equation (15) after substitution for s_1 and s_2 becomes,

$$\psi_n(t) = e^{\beta_n t}\{C_{1n}\sinh[\sqrt{\beta_n^2-\gamma_n^2}\,t] + C_{2n}\cosh[\sqrt{(\beta_n^2-\gamma_n^2)}\,t]\} + \int_0^t \frac{e^{\beta_n(t-\tau)}\sinh[\sqrt{\beta_n^2-\gamma_n^2}(t-\tau)]}{\sqrt{\beta_n^2-\gamma_n^2}}g_n^*(\tau)\,d\tau \quad \text{when } \beta_n^2-\gamma_n^2 > 0. \quad (16)$$

Depending on the sign of the quantity $(\beta_n^2-\gamma_n^2)$, the arguments of the hyperbolic sine and cosine in equation (16) will be real or imaginary. The temperature solution is obtained by substituting $\psi_n(t)$ from equation (16) in equation (6):

$$T(\mathbf{r},t) = T^*(\mathbf{r},t) + \sum_{n=1}^{\infty} F_n(\mathbf{r})e^{-\gamma_n t}e^{\beta_n t}\{C_{1n}\sinh[\sqrt{\beta_n^2-\gamma_n^2}\,t] + C_{2n}\cosh[\sqrt{\beta_n^2-\gamma_n^2}\,t]\} + \sum_{n=1}^{\infty} F_n(\mathbf{r})e^{-\gamma_n t} \times \int_0^t \frac{e^{\beta_n(t-\tau)}\sinh[\sqrt{\beta_n^2-\gamma_n^2}(t-\tau)]}{\sqrt{\beta_n^2-\gamma_n^2}}g_n^*(\tau)\,d\tau. \quad (17)$$

Equation (17) is the solution of equation (1). As demonstrated by examining equation (17), the general solution is the sum of three effects: initial conditions, T_0, internal heat source, T_G, and boundary conditions, T_B. For convenience, the solution is written as

$$T(\mathbf{r},t) = T_0(\mathbf{r},t) + T_G(\mathbf{r},t) + T_B(\mathbf{r},t) \quad (18)$$

and each of the three functions is described separately.

The effect of the initial conditions is examined using the following terms in equation (17):

$$T_0(\mathbf{r},t) = \sum_{n=1}^{\infty} F_n(\mathbf{r})e^{-\gamma_n t}e^{\beta_n t}\{C_{1n}\sinh[\sqrt{\beta_n^2-\gamma_n^2}\,t] + C_{2n}\cosh[\sqrt{\beta_n^2-\gamma_n^2}\,t]\}. \quad (19)$$

Two initial conditions are needed to compute C_{1n} and C_{2n}. The first initial condition, $T_0(\mathbf{r},0) = T(\mathbf{r},0) - T^*(\mathbf{r},0) = T_i(\mathbf{r})$, equation (19), after using the orthogonality condition, equation (8), yields

$$C_{2n} = \frac{1}{N_n}\int_V T_i(\mathbf{r}')F_n(\mathbf{r}')\,dV'. \quad (20)$$

Applying the second initial condition $[\partial T_0(\mathbf{r},t)/\partial t]_{t=0} = [\partial T(\mathbf{r},t)/\partial t - \partial T^*(\mathbf{r},t)/\partial t]_{t=0} = T_{ii}(\mathbf{r})$ to equation (19) and following the application of the orthogonality condition one obtains

$$C_{1n} = \frac{1}{N_n\sqrt{\beta_n^2-\gamma_n^2}}\int_V T_{ii}(\mathbf{r}')F_n(\mathbf{r}')\,\mathrm{d}V' + \frac{\sigma^2/2\alpha}{\sqrt{\beta_n^2-\gamma_n^2}}C_{2n}. \quad (21)$$

Equations (19), (20), and (21) can be combined into the following single equation:

$$T_0(\mathbf{r},t) = \int_V \sum_{n=1}^{\infty}\frac{F_n(\mathbf{r})F_n(\mathbf{r}')}{N_n}\mathrm{e}^{-\gamma_n t}\mathrm{e}^{\beta_n t} \times \left\{T_i(\mathbf{r}')\cosh[\sqrt{\beta_n^2-\gamma_n^2}\,t] + \frac{\sinh[\sqrt{\beta_n^2-\gamma_n^2}\,t]}{\sqrt{\beta_n^2-\gamma_n^2}} \times\left[\frac{\sigma^2}{2\alpha}T_i(\mathbf{r}')+T_{ii}(\mathbf{r}')\right]\right\}\mathrm{d}V'. \quad (22)$$

Equation (22) holds for the conditions $\beta_n^2-\gamma_n^2 > 0$ and $\beta_n^2-\gamma_n^2 < 0$. When $\beta_n^2-\gamma_n^2 < 0$, the following identities apply:

$$\cosh[\sqrt{\beta_n^2-\gamma_n^2}\,t] = \cos[\sqrt{\gamma_n^2-\beta_n^2}\,t]$$
$$\frac{\sinh[\sqrt{\beta_n^2-\gamma_n^2}\,t]}{\sqrt{\beta_n^2-\gamma_n^2}} = \frac{\sin[\sqrt{\gamma_n^2-\beta_n^2}\,t]}{\sqrt{\gamma_n^2-\beta_n^2}}. \quad (23)$$

For the evaluation of $T_G(\mathbf{r},t)$ in equation (18), consider the case when the source term does not have a zero value. The function $T_G(\mathbf{r},t)$, equation (18), accounts for the contribution of $\bar{g}(\mathbf{r}',\tau)$ to $g_n^*(\tau)$ in equation (17). The contribution of volumetric heat source using equations (2), (11), and (17) is

$$T_G(\mathbf{r},t) = \sum_{n=1}^{\infty}F_n(\mathbf{r})\mathrm{e}^{-\gamma_n t} \times\int_0^t \frac{\mathrm{e}^{\beta_n(t-\tau)}\sinh[\sqrt{\beta_n^2-\gamma_n^2}(t-\tau)]}{\sqrt{\beta_n^2-\gamma_n^2}}\frac{\sigma^2\mathrm{e}^{\gamma_n\tau}}{kN_n} \times\int_V F_n(\mathbf{r}')\left[g(\mathbf{r}',\tau)+\frac{\alpha}{\sigma^2}\frac{\partial g(\mathbf{r}',\tau)}{\partial\tau}\right]\mathrm{d}V'\,\mathrm{d}\tau. \quad (24)$$

Equation (24) equally holds when $\beta_n^2-\gamma_n^2 > 0$ or $\beta_n^2-\gamma_n^2 < 0$; see equation (23).

The function $T_B(\mathbf{r},t)$ is the contribution of the boundary conditions to the temperature solution. The function $T_B(\mathbf{r},t)$ consists of the terms that contain $T^*(\mathbf{r},t)$ in equation (17) and the definition of $g_n^*(\tau)$ using equation (11). Then, the contribution of non-homogeneous boundary conditions, $T_B(\mathbf{r},t)$, is

$$T_B(\mathbf{r},t) = T^*(\mathbf{r},t)+\sum_{n=1}^{\infty}F_n(\mathbf{r})\mathrm{e}^{-\gamma_n t} \times\int_0^t \frac{\mathrm{e}^{\beta_n(t-\tau)}\sinh[\sqrt{\beta_n^2-\gamma_n^2}(t-\tau)]}{\sqrt{\beta_n^2-\gamma_n^2}}\frac{\sigma^2\mathrm{e}^{\gamma_n\tau}}{kN_n} \times\int_V F_n(\mathbf{r}')\left[\nabla\cdot[k\nabla T^*(\mathbf{r}',\tau)]-\rho c_p\frac{\partial T^*(\mathbf{r}',\tau)}{\partial\tau} - \frac{k}{\sigma^2}\left[\frac{\partial^2 T^*(\mathbf{r}',\tau)}{\partial\tau^2}\right]\right]\mathrm{d}V'\,\mathrm{d}\tau. \quad (25)$$

If T^* is the steady-state solution, then $\nabla\cdot[k\nabla T^*(\mathbf{r})] = 0$ and $\rho c_p\partial T^*(\mathbf{r})/\partial t = 0$. However, it is possible to have $\nabla\cdot[k\nabla T^*(\mathbf{r},t)] = 0$ while $\partial T^*(\mathbf{r},t)/\partial t \neq 0$.

The substitution of equations (22), (24), and (25) in equation (18) represents the solution of the thermal wave equation. This solution uses the eigenfunctions of the solution for the Fourier-type heat conduction. Since solutions of the Fourier-type heat conduction for various finite bodies are available [6, 7], equation (18) yields the solution of the thermal wave form of heat conduction.

The procedure developed here leads to the development of a methodology that is based on the Green's function solution method. The Green's function solution method is a better and simpler procedure to obtain a solution for a thermal wave equation. The objective is to develop a solution technique for the thermal wave equation that uses the already available tabulated Green's functions [6] for the Fourier-type conduction equation. To present the solutions in terms of universally available solutions, it is necessary to define the Green's function. Here, the definition of the Green's function is the same as the definition of the Green's function for Fourier-type conduction. It is the temperature distribution as a function of $\mathbf{r}$ and t when there is a quantity of heat released at point $\mathbf{r}^*$ at time τ^* according to the relation $g(\mathbf{r},t) = \rho c_p\delta(t-\tau^*)\delta(\mathbf{r}-\mathbf{r}^*)$. This leads to a derivation of a Green's function based on existing information available in the literature. The function $\bar{g}(\mathbf{r},t)$ using equation (2) takes the following form:

$$\bar{g}(\mathbf{r},t) = \rho c_p\delta(t-\tau^*)\delta(\mathbf{r}-\mathbf{r}^*) + \rho c_p\delta(\mathbf{r}-\mathbf{r}^*)\frac{\alpha}{\sigma^2}\frac{\partial\delta(t-\tau^*)}{\partial t}. \quad (26)$$

The definition of the Green's function presented here is different from that given by Ozisik and Vick [4] because of the second term on the right-hand side of equation (26).

After differentiating $\delta(t-\tau^*)$ with respect to τ^* instead of t, equation (26) becomes

$$\bar{g}(\mathbf{r},t) = \rho c_p\delta(t-\tau^*)\delta(\mathbf{r}-\mathbf{r}^*) - \rho c_p\delta(\mathbf{r}-\mathbf{r}^*)\frac{\alpha}{\sigma^2}\frac{\partial\delta(t-\tau^*)}{\partial\tau^*}. \quad (27)$$

Equation (24) provides the Green's function when $\bar{g}(\mathbf{r},t)$ is given by equation (27). One must replace $\mathbf{r}$ by $\mathbf{r}'$ and t by τ in $\bar{g}(\mathbf{r},t)$ and then substitute $\bar{g}(\mathbf{r}',\tau)$ in equation (24) to obtain

$$T_G(\mathbf{r},t) = \sum_{n=1}^{\infty}F_n(\mathbf{r})\mathrm{e}^{-\gamma_n t} \times\int_0^t \frac{\mathrm{e}^{\beta_n(t-\tau)}\sinh[\sqrt{\beta_n^2-\gamma_n^2}(t-\tau)]}{\sqrt{\beta_n^2-\gamma_n^2}}\times\frac{\sigma^2 e^{\gamma_n\tau}}{kN_n} \times\int_V F_n(\mathbf{r}')\Big[\rho c_p\delta(\tau-\tau^*)\delta(\mathbf{r}'-\mathbf{r}^*)$$

$$-\rho c_p \delta(\mathbf{r}'-\mathbf{r}^*)\frac{\alpha}{\sigma^2}\frac{\partial\delta(\tau-\tau^*)}{\partial\tau^*}\Bigg] \mathrm{d}V'\,\mathrm{d}\tau$$

$$= \sum_{n=1}^{\infty}\frac{F_n(\mathbf{r})}{N_n}\left(\int_V F_n(\mathbf{r}')\delta(\mathbf{r}'-\mathbf{r}^*)\,\mathrm{d}V'\right)$$

$$\times\left\{\left(\frac{\sigma^2}{\alpha}\int_0^t \frac{\exp[-(\gamma_n-\beta_n)(t-\tau]\sinh[\sqrt{\beta_n^2-\gamma_n^2}(t-\tau)]}{\sqrt{\beta_n^2-\gamma_n^2}}\right.\right.$$

$$\left.\times\,\delta(\tau-\tau^*)\,\mathrm{d}\tau\right)-\frac{\partial}{\partial\tau^*}$$

$$\times\left(\int_0^t \frac{\exp[-(\gamma_n-\beta_n)(t-\tau)]\sinh[\sqrt{\beta_n^2-\gamma_n^2}(t-\tau)]}{\sqrt{\beta_n^2-\gamma_n^2}}\right.$$

$$\left.\left.\times\,\delta(\tau-\tau^*)\,\mathrm{d}\tau\right)\right\}. \qquad (28)$$

Following integration of equation (28) using the standard delta function identities, subsequent differentiation with respect to τ^*, and some algebra that uses the definition of β_n in equation (10), one obtains

$$T_G(\mathbf{r},t) = \sum_{n=1}^{\infty}\frac{F_n(\mathbf{r})F_n(\mathbf{r}')}{N_n}\mathrm{e}^{-\gamma_n(t-\tau)}$$

$$\times\left(\mathrm{e}^{\beta_n(t-\tau)}\frac{\sinh[\omega_n(t-\tau)]}{2\alpha\omega_n/\sigma^2}\right)+\sum_{n=1}^{\infty}\frac{F_n(\mathbf{r})F_n(\mathbf{r}^*)}{N_n}\mathrm{e}^{-\gamma_n(t-\tau^*)}$$

$$\times\{\mathrm{e}^{\beta_n(t-\tau^*)}\cosh[\sqrt{\beta_n^2-\gamma_n^2}(t-\tau^*)]\}. \quad (29)$$

The function $T_G(\mathbf{r},t)$ is the temperature at point $\mathbf{r}$ and time t when there is an energy $g(\mathbf{r},t) = \rho c_p\delta(t-\tau^*)\delta(\mathbf{r}-\mathbf{r}^*)$ at point $\mathbf{r}^*$ released at time τ^*. Accordingly $T_G(\mathbf{r},t)$ represents the Green's function computed for the wave-type conduction equation. After replacing τ^* by τ and $\mathbf{r}^*$ by $\mathbf{r}'$, the function $T_G(\mathbf{r},t)$ will be designated as $G_w(\mathbf{r},t|\mathbf{r}',\tau)$, that is,

$$G_w(\mathbf{r},t|\mathbf{r}',\tau) = G_{wa}(\mathbf{r},t|\mathbf{r}',\tau)+G_{wb}(\mathbf{r},t|\mathbf{r}',\tau) \quad (30)$$

where

$$G_{wa}(\mathbf{r},t\,|\,\mathbf{r}',\tau) = \sum_{n=1}^{\infty}\frac{F_n(\mathbf{r})F_n(\mathbf{r}')}{N_n}$$

$$\times\,\mathrm{e}^{-\gamma_n(t-\tau)}\left\{\mathrm{e}^{\beta_n(t-\tau)}\frac{\sinh[\omega_n(t-\tau)]}{2\alpha\omega_n/\sigma^2}\right\} \quad (31)$$

and

$$G_{wb}(\mathbf{r},t\,|\,\mathbf{r}',\tau) = \sum_{n=1}^{\infty}\frac{F_n(\mathbf{r})F_n(\mathbf{r}')}{N_n}$$

$$\times\,\mathrm{e}^{-\gamma_n(t-\tau)}\{\mathrm{e}^{\beta_n(t-\tau)}\cosh[\omega_n(t-\tau)]\} \quad (32)$$

where $\omega_n = \sqrt{\beta_n^2-\gamma_n^2}$ and $2\alpha\omega_n/\sigma^2 = \sqrt{1-4\gamma_n\alpha/\sigma^2}$. The wave form of the Green's function, equation (30), has two conjugate components: an a-conjugate component and a b-conjugate component. The b-conjugate component is useful for calculating the contribution of the initial condition. Except for the terms in curly brackets, the definitions for $G_{wa}(\mathbf{r},t\,|\,\mathbf{r}',\tau)$ and $G_{wb}(\mathbf{r},t\,|\,\mathbf{r}',\tau)$ are the same as the definition for the standard Green's function for the diffusion equation

$$G(\mathbf{r},t\,|\,\mathbf{r}',\tau) = \sum_{n=1}^{\infty}\frac{F_n(\mathbf{r})F_n(\mathbf{r}')}{N_n}\mathrm{e}^{-\gamma_n(t-\tau)}. \quad (33)$$

A comparison between equation (33) and equations (31) and (32) shows that these equations have an identical form. A Green's function using equation (33) is chosen as the referenced quantity because, for a given problem, it can be inferred from the universally available Green's functions for Fourier-type conduction [6]. This means that many Green's functions can be simply written down using the tabulated Green's functions given in ref. [6] and then augmented by the bracketed terms in equations (31) and (32).

Green's function solutions

Equation (22) can be written in terms of the Green's function components $G_{wa}(\mathbf{r},t\,|\,\mathbf{r}',\tau)$ and $G_{wb}(\mathbf{r},t\,|\,\mathbf{r}',\tau)$:

$$T_0(\mathbf{r},t) = \int_V\Bigg[T_i(\mathbf{r}')G_w(\mathbf{r},t\,|\,\mathbf{r}',0)$$

$$+\frac{2\alpha}{\sigma^2}T_{ii}(\mathbf{r}')G_{wa}(\mathbf{r},t\,|\,\mathbf{r}',0)\Bigg]\mathrm{d}V'. \quad (34)$$

Except for the term corresponding to $T_{ii}(\mathbf{r}')$, equation (34) is similar to the corresponding Green's function solution for Fourier-type heat conduction. Similarly, equation (24) can be written in the form that uses the Green's functions for the Fourier heat conduction as

$$T_G(\mathbf{r},t) = \frac{2\alpha}{k}\int_0^t \mathrm{d}\tau\int_V G_{wa}(\mathbf{r},t\,|\,\mathbf{r}',\tau)\bar{g}(\mathbf{r},'\tau)\,\mathrm{d}V' \quad (35)$$

where $\bar{g}(\mathbf{r}',\tau)$ is given by equation (2). The contribution of the heat source in the Fourier-type heat conduction is quite similar to equation (35). Here, in addition to a factor of 2, the a-conjugate component of the Green's function is used while the source term in equation (35) is represented by $\bar{g}(\mathbf{r}',\tau)$ instead of $g(\mathbf{r}',\tau)$.

For the contribution of the boundary conditions, equation (25) using the Green's function, equation (31), is

$$T_B(\mathbf{r},t) = T^*(\mathbf{r},t)+\frac{2\alpha}{k}\int_{\tau=0}^t \mathrm{d}\tau$$

$$\times\int_V G_{wa}(\mathbf{r},t\,|\,\mathbf{r}',\tau)\Bigg[\nabla\cdot[k\nabla T^*(\mathbf{r}',\tau)]-\rho c_p\frac{\partial T^*(\mathbf{r}',\tau)}{\partial\tau}$$

$$-\frac{k}{\sigma^2}\left[\frac{\partial^2 T^*(\mathbf{r}',\tau)}{\partial\tau^2}\right]\Bigg]. \quad (36)$$

Equation (36) is analogous to the alternative Green's function solution defined in ref. [6]. When a T^* function is not readily available, it is possible to set

$$T^*(\mathbf{r},t) = \alpha\int_0^t d\tau\int_S\left[G(\mathbf{r},t\,|\,\mathbf{r}',\tau)\frac{\partial T(\mathbf{r}',\tau)}{\partial n} - T(\mathbf{r}',\tau)\frac{\partial G(\mathbf{r},t\,|\,\mathbf{r}',\tau)}{\partial n}\right]_{S'} dS'. \quad (37)$$

This form of T^* causes the term $\nabla\cdot[k\nabla T^*(\mathbf{r},t)] - \rho c_p[\partial T^*(\mathbf{r},t)/\partial t]$ to become zero. However, this is not recommended because the convergence of equation (35) is poor when $G(\mathbf{r},t\,|\,\mathbf{r}',\tau)$ is an infinite series. In some cases, it is preferred to solve the Laplace equation $\nabla\cdot[k\nabla T^*(\mathbf{r},t)] = 0$ using the non-homogeneous boundary condition and treating time, t, as a parameter. Equation (36) yields the value of T_B, while the terms containing $\partial T^*(\mathbf{r}',\tau)/\partial\tau$ and $\partial^2 T^*(\mathbf{r}',\tau)/\partial\tau^2$ are retained.

As stated earlier, the Green's function is readily available for many problems. Since the substitution of equations, (34), (35), and (46) in equation (18) yields the temperature, the lengthy algebraic steps described in this paper need not be repeated.

Transition to diffusion equation

It is now shown that the thermal conduction described by the wave equation reduces to the solution for the diffusion equation. The task is simplified by proving that equation (30), as $\sigma\to\infty$, reduces to the corresponding Green's function equation for the standard thermal diffusion; that is,

$$\lim_{\sigma\to\infty} G_{wa}(\mathbf{r},t\,|\,\mathbf{r}',\tau) = \tfrac{1}{2}G(\mathbf{r},t\,|\,\mathbf{r}',\tau) \quad (38a)$$

and

$$\lim_{\sigma\to\infty} G_{wb}(\mathbf{r},t\,|\,\mathbf{r}',\tau) = \tfrac{1}{2}G(\mathbf{r},t\,|\,\mathbf{r}',\tau). \quad (38b)$$

These two limiting values can be shown if

$$\lim_{\sigma\to\infty}\left[e^{\beta_n(t-\tau)}\frac{\sinh[\omega_n(t-\tau)]}{2\alpha\omega_n/\sigma^2}\right] = \tfrac{1}{2} \quad (39a)$$

and

$$\lim_{\sigma\to\infty}[e^{\beta_n(t-\tau)}\cosh[\omega_n(t-\tau)]] = \tfrac{1}{2}. \quad (39b)$$

Proof. Using β_n defined in equation (10), ω_n reduces to

$$\omega_n = \sqrt{\beta_n^2-\gamma_n^2} = \left(\frac{\sigma^2}{2\alpha}\right)\sqrt{1-4\gamma_n\alpha/\sigma^2}. \quad (40)$$

This equation, following expansion using the binomial series, becomes

$$\omega_n = \left(\frac{\sigma^2}{2\alpha}\right)\left[1-\frac{1}{2}\frac{4\gamma_n\alpha}{\sigma^2}-\frac{1/4}{2!}\left(\frac{4\gamma_n\alpha}{\sigma^2}\right)^2-\cdots\right]. \quad (41)$$

For large σ, one can assume $4\gamma_n\alpha/\sigma^2 \ll 1$. Retaining the first two terms in square brackets in equation (41) and replacing all remaining terms by $E(\sigma)$, the function ω_n becomes

$$\omega_n = \left(\frac{\sigma^2}{2\alpha}\right)-\gamma_n+E(\sigma) \quad (42)$$

where $E(\sigma)\to 0$ as $\sigma\to\infty$. Equation (39a) can be rewritten as

$$\lim_{\sigma\to\infty}\frac{\sigma^2}{4\omega_n\alpha}\{\exp[(\beta_n+\omega_n)(t-\tau)] - \exp[(\beta_n-\omega_n)(t-\tau)]\} = \tfrac{1}{2}. \quad (43a)$$

According to the definition, $\beta_n = \gamma_n-\sigma^2/2\alpha$, equation (10), and ω_n in equation (42), the following quantities in equation (43a) are calculated: $\sigma^2/(4\omega_n\alpha) = (\sigma^2/4\alpha)/[(\sigma^2/2\alpha)-\gamma_n+E(\sigma)]$, $\beta_n+\omega_n = E(\sigma)$, $\beta_n-\omega_n = 2(\gamma_n-\sigma^2/2\alpha)-E(\sigma)$. When $\sigma\to\infty$, then $\sigma^2/(4\omega_n\alpha)\to 1/2$, $\beta_n+\omega_n\to 0$, and $\beta_n-\omega_n\to-\infty$. Therefore, the first term in the curly brackets in equation (43a) approaches 1 and the second term in the curly brackets becomes zero. Similarly, equation (39b) reduces to

$$\lim_{\sigma\to\infty}\tfrac{1}{2}[\exp(\beta_n+\omega_n)(t-\tau)] + \exp[(\beta_n-\omega_n)(t-\tau)] = \tfrac{1}{2} \quad (43b)$$

This proves that equations (39a) and (39b) are correct.

At the limit when $\sigma\to\infty$, the identities given by equations (39a) and (39b) will force the terms on the right-hand side of equation (30) to become $\lim_{\sigma\to\infty} G_{wa}(\mathbf{r},t|\mathbf{r}',\tau) = (1/2)G(\mathbf{r},t|\mathbf{r}',\tau)$ and $\lim_{\sigma\to\infty} G_{wb}(\mathbf{r},t|\mathbf{r}',\tau) = (1/2)G(\mathbf{r},t|\mathbf{r}',\tau)$. Accordingly, the solutions for the wave form of the diffusion equation will reduce to the solutions for the standard diffusion equation as $\sigma\to\infty$.

Example 1

The objective of this example is to formulate the Green's function for a slab insulated on both sides and to provide numerical values. The one-dimensional example compares the mathematical derivation presented in this paper with the work of Ozisik and Vick [4].

Solution. The Green's function for Fourier-type conduction (X22 in ref. [6], p. 492) can be written as

$$G(x,t\,|\,x',\tau) = \frac{1}{L}\left[1+2\sum_{m=1}^{\infty}\exp[-m^2\pi^2\alpha(t-\tau)/L^2 \times\cos\left(\frac{m\pi x}{L}\right)\cos\left(\frac{m\pi x'}{L}\right)\right]. \quad (44)$$

Comparing this equation with equation (33), the first eigenvalue is $\gamma_1 = 0$. The remaining eigenvalues are: $\gamma_2 = \pi^2\alpha/L^2$, $\gamma_3 = 2^2\pi^2\alpha/L^2,\ldots$, $\gamma_n = (n-1)^2\pi^2\alpha/L^2$. Also, the eigenfunctions are $F_n(\mathbf{r}) = \cos[(n-1)\pi x/L]$ and $F_n(\mathbf{r}') = \cos[(n-1)\pi x'/L]$, and the norms are $N_1 = L$ and $N_n = L/2$ for $n>1$. Equation (44) can be written as

$$G(x,t\,|\,x',\tau) = \sum_{m=0}^{\infty}\frac{2-\delta_{0m}}{L}\cos\left(\frac{m\pi x}{L}\right)\times\cos\left(\frac{m\pi x'}{L}\right)\exp[-m^2\pi^2\alpha(t-\tau)/L^2] \quad (45)$$

where δ_{0m} is the Kronecker delta, $\delta_{0m} = 1$ when $m = 0$ and $\delta_{0m} = 0$ when $m \neq 0$. The a-conjugate and b-conjugate components of the Green's function are simply obtained by multiplying equation (45) by the terms in the curly brackets of equations (31) and (32). The results are

$$G_{wa}(x,t|x',\tau) = \sum_{m=0}^{\infty} \frac{2-\delta_{0m}}{L} \cos\left(\frac{m\pi x}{L}\right) \times \cos\left(\frac{m\pi x'}{L}\right) \exp[-m^2\pi^2\alpha(t-\tau)/L^2] \times \left[e^{\beta_m(t-\tau)} \frac{\sinh[\omega_m(t-\tau)]}{2\alpha\omega_m/\sigma^2}\right] \quad (46a)$$

and

$$G_{wb}(x,t\,|\,x',\tau) = \sum_{m=0}^{\infty} \frac{2-\delta_{0m}}{L} \cos\left(\frac{m\pi x}{L}\right) \times \cos\left(\frac{m\pi x'}{L}\right) \exp[-m^2\pi^2\alpha(t-\tau)/L^2] \times [e^{\beta_m(t-\tau)} \cosh[\omega_m(t-\tau)]] \quad (46b)$$

where

$$\beta_m = m^2\pi^2\alpha/L^2 - \sigma^2/2\alpha$$

and

$$\omega_m = \sqrt{\beta_m^2 - (m^2\pi^2\alpha/L^2)^2}.$$

The sum of equations (46a) and (46b) gives the value of the Green's function for the thermal wave equation, as indicated by equation (30). The parameter $\sigma L/\alpha$ is the dimensionless wave speed. A one-dimensional solution, for a pulse with finite thickness, as reported in ref. [4], will reduce to the Green's function given by the sum of equations (46a) and (46b).

An examination of equations (46a) or (46b) shows that exponential terms may be combined and written as $\exp[-(\sigma^2/2\alpha)(t-\tau)]$ which is independent of m and will not contribute to the convergence of the solution. Therefore, the convergence of equation (46b), in particular, is expected to be slow. However, when $\sigma L/\alpha$ is large, the terms in the large square bracket, equations (46a) or (46b), will approach $\frac{1}{2}$, equations (39a) and (39b), and the convergence will be similar to that for the classical Green's function in diffusion problems. Figure 1(a) shows the rate of convergence for $G(\cdot)$, $G_{wa}(\cdot)$, $G_{wb}(\cdot)$, and $G_w(\cdot)$. The a-conjugate component of the thermal wave equation converges reasonably fast, but slower than the convergence of the Green's function for Fourier conduction, $G(\cdot)$, equation (45). The b-conjugate component has a large contribution to the value of $G_w(\cdot)$ and it did not converge after 60 terms. Figure 1(b) shows $G_w(\cdot) = G_{wa}(\cdot) + G_{wb}(\cdot)$ after 100 terms, 10 000 terms, and 1 000 000 terms. Figure 1(b) indicates that equation (46b) oscillates about the solution and does not converge to the solution.

One can modify equation (46b) and achieve a relatively fast convergence for $G_w(\cdot)$ by extracting the contribution of the energy pulse, represented by the delta function, from this solution. For instance, at the limit when $c_p \to 0$ one obtains $\omega_m \to im\pi\sigma/L$, indicating that the material domain does not have a capacity to store thermal energy. For the zero-heat-capacity condition, $\alpha \to \infty$, equation (46b) reduces to a solution for an energy pulse moving in the material domain and reflecting from the walls. Using the expansion of the delta function in the Fourier cosine series, the right-hand side of equation (46b), for the case of $\alpha \to \infty$, reduces to

$$\sum_{m=0}^{\infty} \frac{2-\delta_{0m}}{L} \cos\left(\frac{m\pi x}{L}\right) \cos\left(\frac{m\pi x'}{L}\right) \cos\left(\frac{m\pi\sigma(t-\tau)}{L}\right) = \frac{1}{2}[\delta((x+x')-\xi) + \delta(|x-x'|-\xi)]$$

where $\xi = |\sigma(t-\tau) - 2jL|$ and j corresponds to the number of reflections from the $x = L$ surface. The value of $j = 0$ before the pulse is reflected or after one reflection from the $x = 0$ surface; the pulse first arrives at x when $\xi = |x-x'|$ and after reflection from the $x = 0$ surface when $\xi = x + x'$. Multiplying both sides of this identity by $\exp[-(\sigma^2/2\alpha)(t-\tau)]$, then adding the resulting relation to equation (46b), yields

$$G_{wb}(x,t\,|\,x',\tau) = \exp[-(\sigma^2/2\alpha)(t-\tau)] \times \left\{\frac{1}{2}[\delta((x+x')-\xi) + \delta(|x-x'|-\xi)] + \sum_{m=0}^{\infty} \frac{2-\delta_{0m}}{L} \cos\left(\frac{m\pi x}{L}\right) \cos\left(\frac{m\pi x'}{L}\right) \times [\cosh(\omega_m(t-\tau)) - \cos(m\pi\sigma(t-\tau)/L)]\right\}. \quad (46c)$$

Figure 1(b) shows that the Green's function, $LG_w(\cdot)$, that uses $G_{wb}(\cdot)$ from equation (46c) sufficiently converges within 100 terms, whereas for a calculation using equation (46b) there is a continuous oscillation about the mean value for a large number of terms. For a faster convergence or when temperature is not a smooth function of position and time, equation (46c) should be used instead of equation (46b). The data are for $\sigma L/\alpha = 10$, $\alpha(t-\tau)/L^2 = 0.025$, and $x/L = 0.2$. The reason for a better convergence, using equation (46b), is that the quantity $\cosh[\omega_m(t-\tau)] - \cos[m\pi\sigma(t-\tau)/L] \to 0$ as $m \to \infty$.

Figure 2 is prepared for $\sigma L/\alpha = 10$. It shows the value of the $LG_w(x,t\,|\,x',\tau)$ as a function of x/L when energy is supplied to the $x = 0$ surface at time τ. The solid lines in the upper portion of the figure, Fig. 2(a), describe the wave front for small times of $\alpha(t-\tau)/L^2 = 0.025$, 0.05, and 0.075. For comparison, the dashed lines represent the solution of the Fourier-type diffusion equation. Notice that early in the diffusion process the difference between the two solutions is quite large.

It is interesting to observe several characteristics of

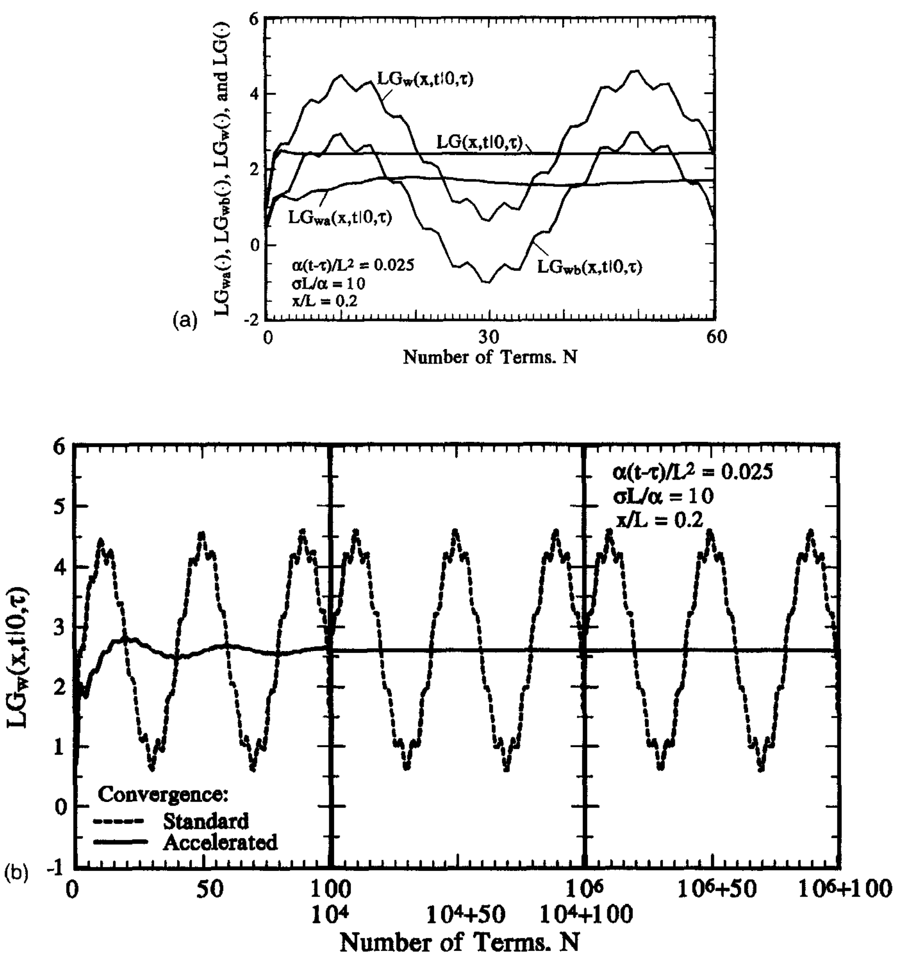

FIG. 1. (a) Convergence of the Green's function for the thermal wave equation and the Green's function for Fourier conduction. (b) Acceleration of the convergence of $G_w(\cdot)$ when $\alpha(t-\tau)/L^2 = 0.025$, $\sigma L/\alpha = 10$, and $x/L = 0.2$

the data shown in Fig. 2(a). It is quite clear that the wave-type conduction and Fourier-type conduction give quite different results, particularly at the smaller times. However, for each of the dimensionless times shown in Fig. 2(a), there is clear evidence of a traveling wave. This has been observed before but these traveling waves have a Dirac-delta-type moving wave at the end location of the wave and their energy is dissipating exponentially as shown by equation (46c). There is no temperature rise beyond that point (for a given time). However, as the strength of the pulse decreases with time, the area under any curve in Fig. 2 remains constant. The bottom portion of this figure, Fig. 2(b), shows the wave front following a reflection from the $x = L$ wall at $\alpha(t-\tau)/L^2 = 0.1$. At $\alpha(t-\tau)/L^2 = 0.125$, the difference between the two solutions becomes small; therefore, the energy remaining in the traveling energy pulse rapidly diminishes as the wave travels toward the $x = 0$ plane.

Figure 3 shows the value of $LG_w(x, t\,|\,x', \tau)$ at $x' = 0$ and $x = 1$ as a function of $\alpha(t-\tau)/L^2$. Each solid line in the figure is for a different value of $\sigma L/\alpha$. The dashed line in Fig. 4 represents $LG(x, t\,|\,x', \tau)$ for Fourier conduction. In this figure, there is a marked difference between the two solutions, especially when $\sigma L/\alpha$ is small. The temperature at $x = L$ remains equal to zero until the arrival of the thermal wave when a jump in temperature occurs. Figure 4 is similar to Fig. 3, except the Green's function is calculated at $x = 0$ instead of $x = L$. Each curve in Fig. 4 includes one reflected pulse after the thermal wave leaves the $x = L$ surface. However, pulses that have been reflected more than once are deleted from the graph. Generally, the series solution representing the Green's function converges slowly for small $\sigma L/\alpha$ values.

Example 2

The purpose of this example is to show the method of determining the Green's function for a multidimensional body.

Solution. A two-dimensional case is used mainly to show the procedure for writing down a solution from existing information available in the literature. Only the mathematical formulation of the Green's function

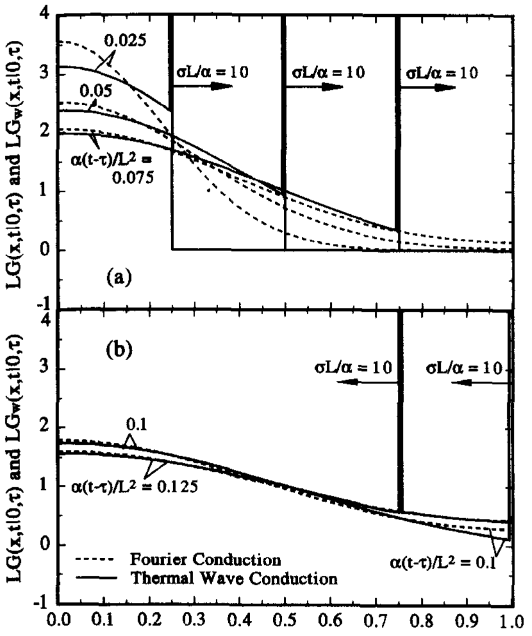

FIG. 2. (a) Forward moving thermal wave at different times. (b) Reflected thermal wave at different times.

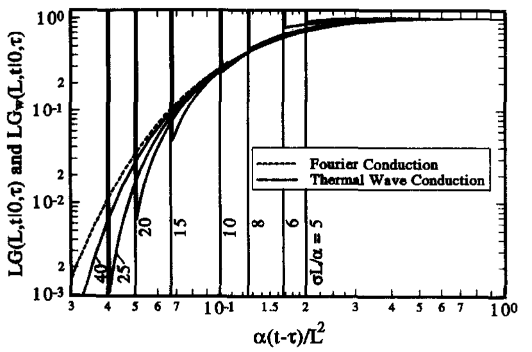

FIG. 3. The effect of thermal wave speed on temperature at $x = L$ plane.

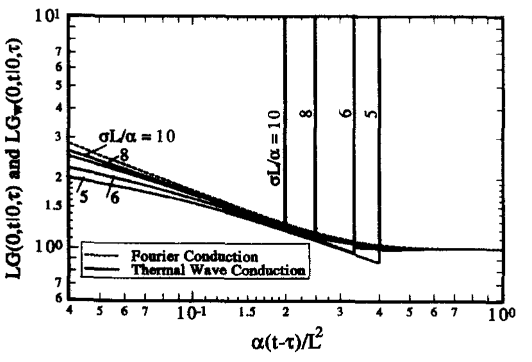

FIG. 4. The effect of thermal wave speed on temperature at $x = 0$ plane.

is presented. This example is concerned with a cylindrical sector of radius b within $0 \leqslant \phi \leqslant \phi_0$; $G = 0$ at $r = b$, $\phi = 0$, and $\phi = \phi_0$. The Green's function for the Fourier-type conduction is (R01Φ11 in ref. [6], p. 453)

$$G(r, \phi, t \mid r', \phi', \tau) = \frac{4}{b^2 \phi_0} \sum_{m=0}^{\infty} \sum_{v}^{\infty} \times \frac{J_v(\mu_{mv} r/b) J_v(\mu_{mv} r'/b) \sin(v\phi) \sin(v\phi')}{J_v'^2(\mu_{mv})} \times \exp[-\mu_{mv}^2 \alpha(t-\tau)/b^2] \quad (47)$$

where $v = j\pi/\phi_0$ for $j = 1, 2, 3, \ldots$, and μ_{mv} are roots of $J_v(\mu_{mv}) = 0$. Because the eigenfunctions and norms remain unchanged, the corresponding solutions for $G_{wa}(r, \phi, t \mid r', \phi', \tau)$ and $G_{wb}(r, \phi, t \mid r', \phi', \tau)$ are

$$G_{wa}(r, \phi, t \mid r', \phi', \tau) = \frac{4}{b^2 \phi_0} \sum_{m=0}^{\infty} \sum_{v}^{\infty} \times \frac{J_v(\mu_{mv} r/b) J_v(\mu_{mv} r'/b) \sin(v\phi) \sin(v\phi')}{J_v'^2(\mu_{mv})} \times \exp[-\mu_{mv}^2 \alpha(t-\tau)/b^2] \times \left\{ e^{\beta_{mv}(t-\tau)} \frac{\sinh[\omega_{mv}(t-\tau)]}{2\alpha\omega_{mv}/\sigma^2} \right\} \quad (48a)$$

and

$$G_{wb}(r, \phi, t \mid r', \phi', \tau) = \frac{4}{b^2 \phi_0} \sum_{m=0}^{\infty} \sum_{v}^{\infty} \times \frac{J_v(\mu_{mv} r/b) J_v(\mu_{mv} r'/b) \sin(v\phi) \sin(v\phi')}{J_v'^2(\mu_{mv})} \times \exp[-\mu_{mv}^2 \alpha(t-\tau)/b^2] \{ e^{\beta_{mv}(t-\tau)} \cosh[\omega_{mv}(t-\tau)] \}. \quad (48b)$$

Equations (48a) and (48b) are exactly the same as equation (47) except for the terms in the curly brackets which are simply copied from equations (31) and (32), respectively. The values of parameters β_{mv} and ω_{mv} using equations (10) and (40) are $\beta_{mv} = \mu_{mv}^2 \alpha/b^2 - \sigma^2/2\alpha$ and $\omega_{mv} = \sqrt{\beta_{mv}^2 - (\mu_{mv}^2 \alpha/b^2)^2}$. Then, equations (34), (35), and (36) will provide the complete temperature solution for the thermal wave equation.

Example 3

This numerical example shows the behavior of a three-dimensional temperature solution. It is especially important to examine the numerical behavior of the solution for situations where there is no perfect pulse. A cubical body $L \times L \times L$ with initial conditions $T_i(x, y, z, 0) = \partial T_i(x, y, z, 0)/\partial t = 0$ is selected. All surfaces are insulated except that heat is being released over an area on the $z = 0$ surface, bounded by the lines $x = 0$, $y = 0$, $x = L/2$, and $y = L/2$. The energy released is $q_0 \sin(2\pi\alpha t/L^2)$ for a time period $0 < t < t_0$, where $\alpha t_0/L^2 = 1/2$. A parametric study of the temperature at different times and at two locations is examined.

Solution. The Green's function given by equation (45) is used to construct the Green's function. The Green's function for Fourier conduction, using the product method [6], is

$$G(x,y,x,t\,|\,x',y',z',\tau) = \sum_{l=0}^{\infty}\sum_{m=0}^{\infty}\sum_{p=0}^{\infty} \frac{\cos(l\pi x/L)\cos(l\pi x/L)}{N_l} \times \frac{\cos(m\pi y/L)\cos(m\pi y/L)}{N_m}\frac{\cos(p\pi z/L)\cos(p\pi z/L)}{N_p} \times \exp\{-[(l\pi)^2+(m\pi)^2+(p\pi)^2]\alpha(t-\tau)/L^2\}$$

where the norms N_l, N_m, and N_p are equal to L when the respective l, m, and p are zero and they are equal to $L/2$ when l, m, and p are larger than zero. For this specific problem, the boundary conditions are homogeneous and the initial temperature and its time derivative are zero. Therefore, the temperature solution given by equation (35) includes only the a-conjugate component of the Green's function. Similar to Example 2, the a-conjugate component is

$$G_{wa}(x,y,x,t\,|\,x',y',z',\tau) = \sum_{l=0}^{\infty}\sum_{m=0}^{\infty}\sum_{p=0}^{\infty} \frac{\cos(l\pi x/L)\cos(l\pi x'/L)}{N_l} \times \frac{\cos(m\pi y/L)\cos(m\pi y'/L)}{N_m}\frac{\cos(p\pi z/L)\cos(p\pi z'/L)}{N_p} \times \exp\{-[(l\pi)^2+(m\pi)^2+(p\pi)^2]\alpha(t-\tau)/L^2\} \times \left[e^{\beta_{mv}(t-\tau)}\frac{\sinh[\omega_{lmp}(t-\tau)]}{2\alpha\omega_{lmp}/\sigma^2}\right].$$

The definitions in equations (10) and (40) yield $\beta_{lmp} = [(l\pi)^2+(m\pi)^2+(p\pi)^2]\alpha/L^2-\sigma^2/2\alpha$ and $\omega_{lmp} = \sqrt{\beta^2_{lmp}-(\mu^2_{lmp}\alpha/b^2)^2}$. Equation (35) for this problem reduces to

$$T(x,y,z,t) = \frac{2\alpha}{k}\int_0^t d\tau \int_{z=0}^{L}\int_{y=0}^{0.5L}\int_{x=0}^{0.5L} G_{wa}(x,y,z,t\,|\,x',y',z',\tau) \times \left[q_0\delta(z-0)\sin(2\pi\alpha t/L^2) + \frac{\alpha q_0\delta(z-0)}{\sigma^2}\frac{\partial\sin(2\pi\alpha t/L^2)}{\partial\tau}\right]dx'\,dy'\,dz'.$$

The Dirac delta function is $\delta(z-0) = 0$ when $z \neq 0$ and $\delta(z-0) = 1$ when $z = 0$. The upper limit of integration over τ is t when $t \leqslant t_0$ and t_0 when $t > t_0$. The substitution of the Green's function in this equation yields

$$T(x,y,x,t) = \sum_{l=0}^{\infty}\sum_{m=0}^{\infty}\sum_{p=0}^{\infty} \frac{\cos(l\pi x/L)\sin(l\pi/2)}{l\pi N_l/L} \times \frac{\cos(m\pi y/L)\sin(m\pi/2)}{m\pi N_m/L}\frac{\cos(p\pi z/L)}{N_p} \times \frac{2\alpha q_0}{k}\int_0^t\left[\sin(2\pi\alpha t/L^2)+\frac{2\pi\alpha^2}{L^2\sigma^2}\cos(2\pi\alpha t/L^2)\right] \times \left[\exp[-\sigma^2(t-\tau)/2\alpha]\frac{\sinh[\omega_{lmp}(t-\tau)]}{2\alpha\omega_{lmp}/\sigma^2}\right]d\tau$$

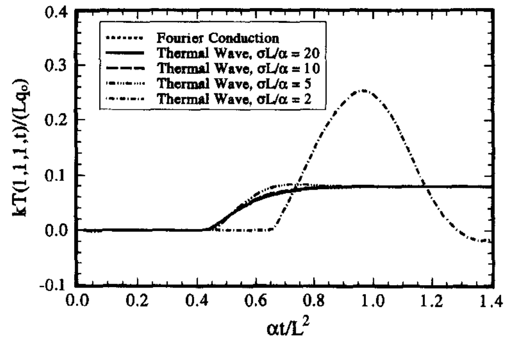

FIG. 5. The effect of thermal wave speed on temperature at point (1, 1, 1).

which reduces to

$$\frac{kT(x,y,x,t)}{Lq_0} = \sum_{l=0}^{\infty}\sum_{m=0}^{\infty}\sum_{p=0}^{\infty} \frac{\cos(l\pi x/L)\sin(l\pi/2)}{l\pi N_l/L} \times \frac{\cos(m\pi y/L)\sin(m\pi/2)}{m\pi N_m/L} \times \frac{\cos(p\pi z/L)}{N_p}\times\frac{2\alpha}{L}\left(I_1+\frac{2\pi\alpha^2}{L^2\sigma^2}I_2\right)$$

where

$$I_1 = \int_0^t \sin(2\pi\alpha t/L^2)\exp[-\sigma^2(t-\tau)/2\alpha] \times \left[\frac{\sinh[\omega_{lmp}(t-\tau)]}{2\alpha\omega_{lmp}/\sigma^2}\right]d\tau$$

and

$$I_2 = \int_0^t \cos(2\pi\alpha t/L^2)\exp[-\sigma^2(t-\tau)/2\alpha] \times \left[\frac{\sinh[\omega_{lmp}(t-\tau)]}{2\alpha\omega_{lmp}/\sigma^2}\right]d\tau.$$

The temperature at the point (1, 1, 1) is plotted in Fig. 5 using $\sigma L/\alpha$ equal to 2, 5, 10, and 20. The value of $\alpha t_0/L^2$ for the data is 0.5. The dashed line in the figure is for the Fourier-type diffusion. The temperature in the thermal wave equation remains equal to zero until the arrival of the wave front. When the dimensionless wave speed is small, e.g. equal to 2, the solution of the thermal wave equation is significantly different. As can be seen from Fig. 5, the wave nature of the solu-

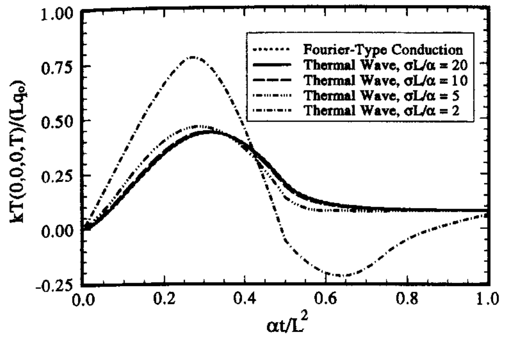

FIG. 6. The effect of thermal wave speed on temperature at point (0, 0, 0).

tion is maintained for a longer period of time. For other dimensionless wave speeds, the solutions approach the equilibrium temperature of $0.24/\pi$ more rapidly. Figure 6 shows the temperature at the point $(0, 0, 0)$ adjacent to the heat source. Here, the characteristic of the solution for small values of the dimensionless wave speed is detectable. The characteristics of the non-equilibrium wave with memory are seen, in particular, for $\sigma L/\alpha = 2$. Figures 5 and 6 show that the sine wave travels in the material domain and slowly loses intensity due to thermal diffusion.

The rate of convergence of the solution of the thermal wave equation is comparable to the solution for Fourier conduction. However, convergence will not happen before the arrival of the wave front. Figure 7 shows the convergence of the thermal wave equation for a different number of terms for the l, m, and p indices. The first set of data in Fig. 7 is for $1 \times 1 \times 1$ terms where the first, second, and third entries correspond to the number of terms used for the l, m, and p indices, respectively. The last entry is for the $35 \times 35 \times 1000$ terms. More terms are used for the summation over the p index because the convergence in the z direction is slower. For instance, the solution using $5 \times 5 \times 5$ terms is different from the case when $35 \times 35 \times 1000$ terms are used, whereas the solutions using $5 \times 5 \times 30$ terms and $35 \times 35 \times 1000$ terms are virtually identical. The computation time using a 486-50 DOS-based personal computer was 10 minutes per temperature data.

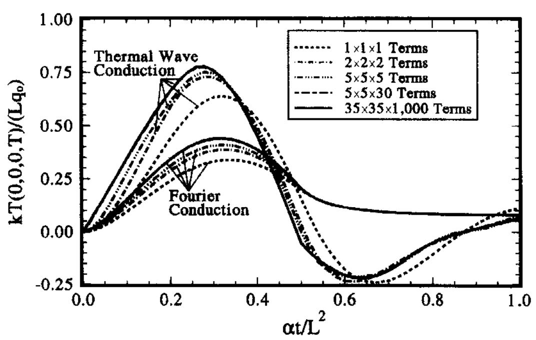

FIG. 7. Convergence of the three-dimensional solution of the thermal wave equation using a different number of terms for dimensionless wave speed $\sigma L/\alpha = 2$.

DISCUSSION

The numerical calculations leading to the derivation of the Green's function solution for the thermal wave equation are lengthy. However, the results are rewarding because the solution of the thermal wave equation in regular finite bodies is now available from existing solutions of the diffusion equation. Examples 2 and 3 show that the temperature solution of the thermal wave equation can be quickly obtained from the tabulated values of the Green's function. The similarity of the solution for the thermal wave conduction and for the Fourier-type conduction by the Green's function method simplifies the method of obtaining solutions to difficult problems. In fact, the solution for many thermal wave problems is readily available if the solution for the corresponding Fourier-type conduction is known. However, the numerical examples show that the convergence of the wave-type conduction solutions is generally poor when the dimensionless wave speed, $\sigma^2/\alpha L$, is small. A series solution with a finite number of terms cannot adequately describe an abrupt change in temperature, e.g. a traveling energy pulse; hence, poor convergence can result, as demonstrated in Example 1. For this reason, it often becomes necessary to employ a convergence-accelerating technique when using a series solution to describe an abrupt change in temperature. A solution to the thermal wave equation may require different strategies to achieve convergence.

This paper opens the door to further investigation of thermal conduction in small structures. The mathematical steps described in this paper transcend the solutions for the thermal wave equation. For example, the procedure described earlier can be used to study the hyperbolic two-step radiation heating model described by Qui and Tien [9]. One can show that the argument of hyperbolic sine and hyperbolic cosine functions for the two-step model are always real; hence, there are no wave-type thermal effects.

Acknowledgement—The work of the first author was partially supported by Texas Advanced Research Program grant number 003656-087.

REFERENCES

1. V. Peshkov, 'Second sound' in helium II, *J. Phys. USSR* **VIII,** 381 (1944).
2. K. J. Baumeister and T. D. Hamill, Hyperbolic heat-conduction equation—a solution for the semi-infinite body problem, *ASME J. Heat Transfer* **91,** 543–548 (1969).
3. K. J. Baumeister and T. D. Hamill, Hyperbolic heat-conduction equation—a solution for the semi-infinite body problem, *ASME J. Heat Transfer* **93,** 126–128 (1971).
4. M. N. Ozisik and B. Vick, Propagation and reflection of thermal waves in a finite medium, *Int. J. Heat Mass Transfer* **27,** 1845–1854 (1984).

5. M. N. Ozisik and D. Y. Tzou, On the wave theory in heat conduction. In *ASME HTD*, Vol. 227 (Edited by Y. Bayazitoglu and G. P. Peterson), pp. 13–27. ASME, New York (1992).
6. J. V. Beck, K. D. Cole, A. Haji-Sheikh and B. Litkouhi, *Heat Conduction Using Green's Functions*. Hemisphere, Washington, DC (1992).
7. H. S. Carslaw and J. C. Jaeger, *Conduction of Heat in Solids* (2nd Edn). Oxford University Press, New York (1959).
8. D. Y. Tzou, Thermal resonance under frequency excitations, *ASME J. Heat Transfer* **114**, 310–316 (1992).
9. T. Q. Qui and C. L. Tien, Heat transfer mechanisms during short-time laser heating of metals, *ASME J. Heat Transfer* **115**, 835–841 (1993).